

## Chapter

# Cell Wall

*Noorah Abdulaziz Othman Alkubaisi  
and Nagwa Mohammed Amin Aref*

## Abstract

The application of AuNPs on the infected barley cultivar had great damage results on Barley Yellow Dwarf Virus (BYDV-PAV) particles in TEM. Observation of TEM images provided an insight into the transport of AuNPs through the plasmodesmata endoplasmic reticulum route, where they likely accumulated as the channels narrowed. The cytoplasmic parenchyma cell components do not have an intact peripheral location, but taking irregular shapes, internal movement between adjacent two cells seems to be the VLPs moved toward via plasmodesmata. TEM micrographs; showing different abnormalities in the cell wall due to viral infection. Application of AuNPs revealed sticky Integrated AuNPs inside the cell wall with low and high density. The mechanical transportation of the virus through the sieve elements with endosomes was observed. The mechanical transportation of virus particles through the cell wall with some vesicles, amorphous inclusions, and filamentous particles was proved through the sieve elements with filamentous strands.

**Keywords:** cell wall, Barley Yellow Dwarf Virus (BYDV-PAV), Gold nanoparticles (AuNPs), parenchyma cells, plasmodesmata, low density of AuNPs, AuNPs with high density, auNPs with high density, twisted cell wall, proteinous contents, endosomes, amorphous inclusions, mechanical transportation, filamentous particles, sieve elements

## 1. Introduction

The phloem-limited virus not only causes damage to the phloem and associated plasmodesmata [1] but also produces viral proteins that influence plasmodesmata structure to allow the passage of viral genomes or virus particles **Figure 1**. Compared to **Figure 2** of healthy cells. For example, the TMV MP accumulates in plasmodesmata and alters the size exclusion limit of the channel [2]. The application of AuNPs on the barley cultivar had great damage results on virus in TEM. The interaction performance in our plates in **Figures 3** and **4** had different degrees between VLPs and AuNPs, illustrated as clotting, surrounding, integration, and accumulation particles. AuNPs with sticky and low density in **Figure 3(A)–(D)** and with high dark density inside the twisted cell wall in **Figure 4(A)–(F)**. The DNA AuNPs can bind to the strand upon entry to the cell's cytoplasm, preventing translation of the mRNAs corresponding protein. As found in **Figure 5(A)** and **(B)**, which pronounced many filamentous strands bind with AuNPs crossing the cell wall, that could have the same influence [3]. Outside of medical technology, the deployment of gold nanoparticles in photovoltaics by embedding them into thin solar cells has increase solar energy conversion efficiencies. The mechanism of AuNPs inside the plant was illustrated [4]. It was recorded that the formation of Nanoparticles still needs more clarification,

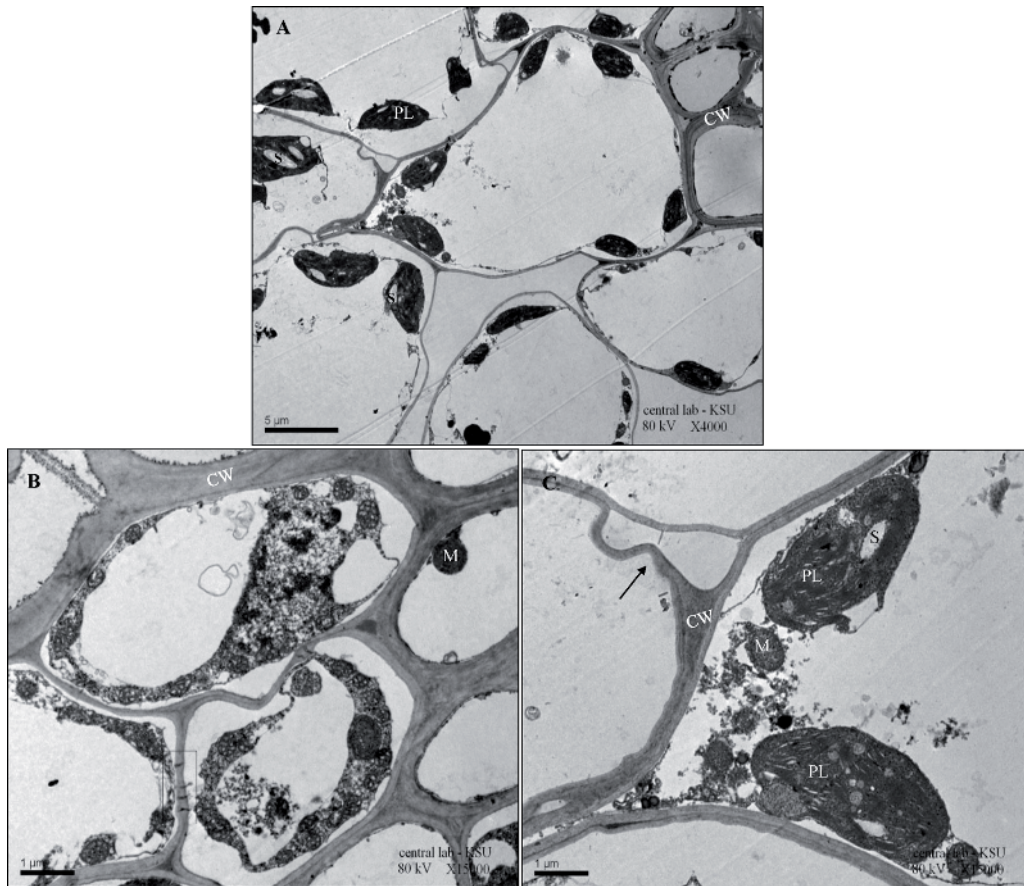


**Figure 1.**

Micrographs of different abnormalities in the cell wall due to viral infection. (A) Parenchyma cells of the entire contents, scale bar 5 µm. (B) The cytoplasmic components do not have an intact peripheral location, but taking irregular shapes internal movement between adjacent two cells, it seems to be the VLPs moved toward via plasmodesmata (outlined), scale bar 1 µm. (C) Increased of the cell wall thickness, irregular wavy cell wall (arrow). Scale bar 1 µm.

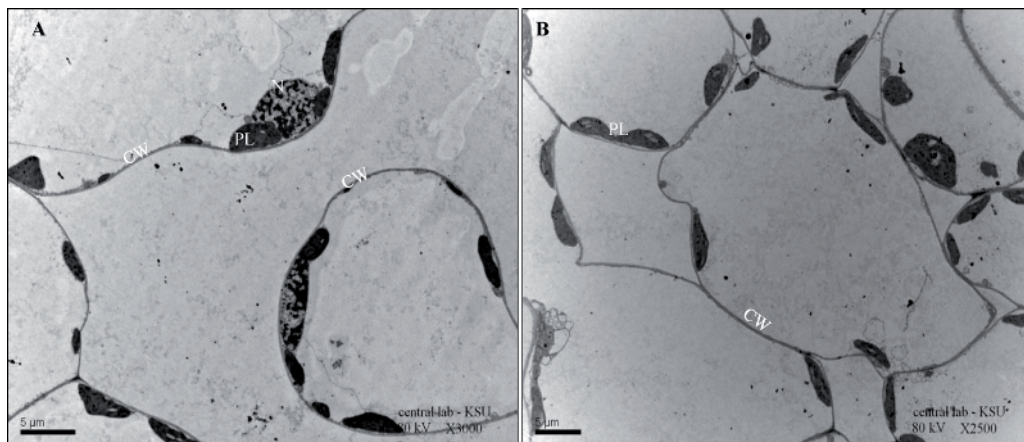


**Figure 2.**

Electron micrographs showing a general view. Healthy cells with different adjacent conducted with the cell wall, as shown in (A and B), scale bars 5 µm.

whether they are created outside and then translocated to plants or whether they are formed by the reduction of metal salts within the plants themselves. The uptake of Nanoparticles and translocation across root cells, in which several active and passive transport processes involved, depends on the type of metal ions and plant

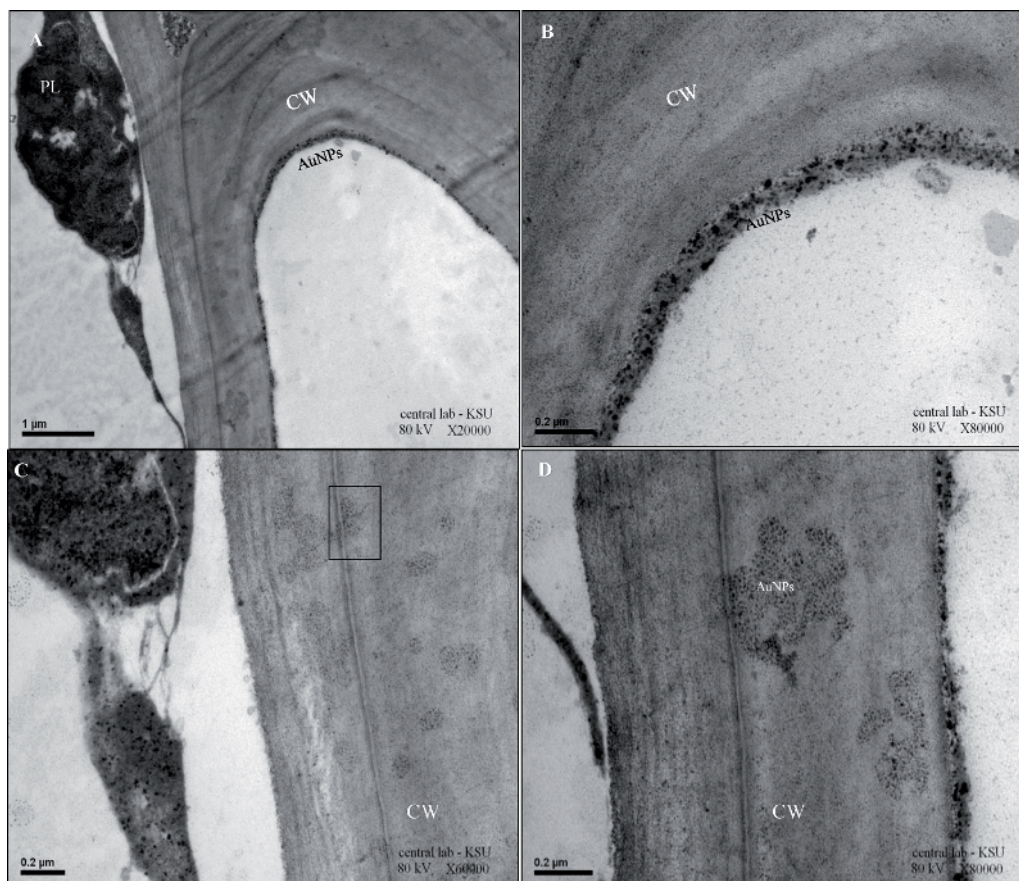


**Figure 3.** Micrographs of the AuNPs sticky and integrated inside the cell wall with low density. (A) AuNPs were gathering together, having large irregular distribution mass net inside the cytoplasm, and circulated the inner side of the cell wall, scale bar 1  $\mu\text{m}$ . (B) Enlarged magnification of A declares AuNPs in the inner border of the cell wall and cytoplasmic area. Scale bar 0.2  $\mu\text{m}$ . (C) AuNPs spotted and attracted firmly on the cell wall (higher magnification of A), scale bar 0.2  $\mu\text{m}$ . (D) Distribution of the AuNPs (higher magnification of C), scale bar 0.2  $\mu\text{m}$ .

species, **Figure 5(A), (B), (E), and (L)**. The amount of Nanoparticle accumulation in plants also varies with the reduction potential of ions and the lowering capacity of plants that depends on the presence of various polyphenols and other heterocyclic compounds present in plants, as shown in **Figure 3(C) and (D)** [5] that sieving properties are determined by the pore diameter of cell wall ranging from 5 to 20 nm **Figure 5(L)**.

## 2. Nanoparticles, interalization and transportation inside the cell wall

During endocytosis, further internalization occurs with a cavity-like structure that forms around the nanoparticles by the plasma membrane. They may, besides, cross the membrane using embedded transport carrier proteins or through ion channels. A band of AuNPs surrounded the cell adjacent and inside the cell wall, as **Figure 5(C)**.

Nuclear Localization Signal Peptide, NLS peptide, is a virus-derived protein fragment [6] that interacts with intracellular proteins for transport across the nuclear envelope. Interpreted that NLS peptides to the DNA AuNP did alter the intercellular localization of the AuNPs [7] but did not change the binding properties of the oligonucleotides (**Figure 5(I), (K) and (M)**).

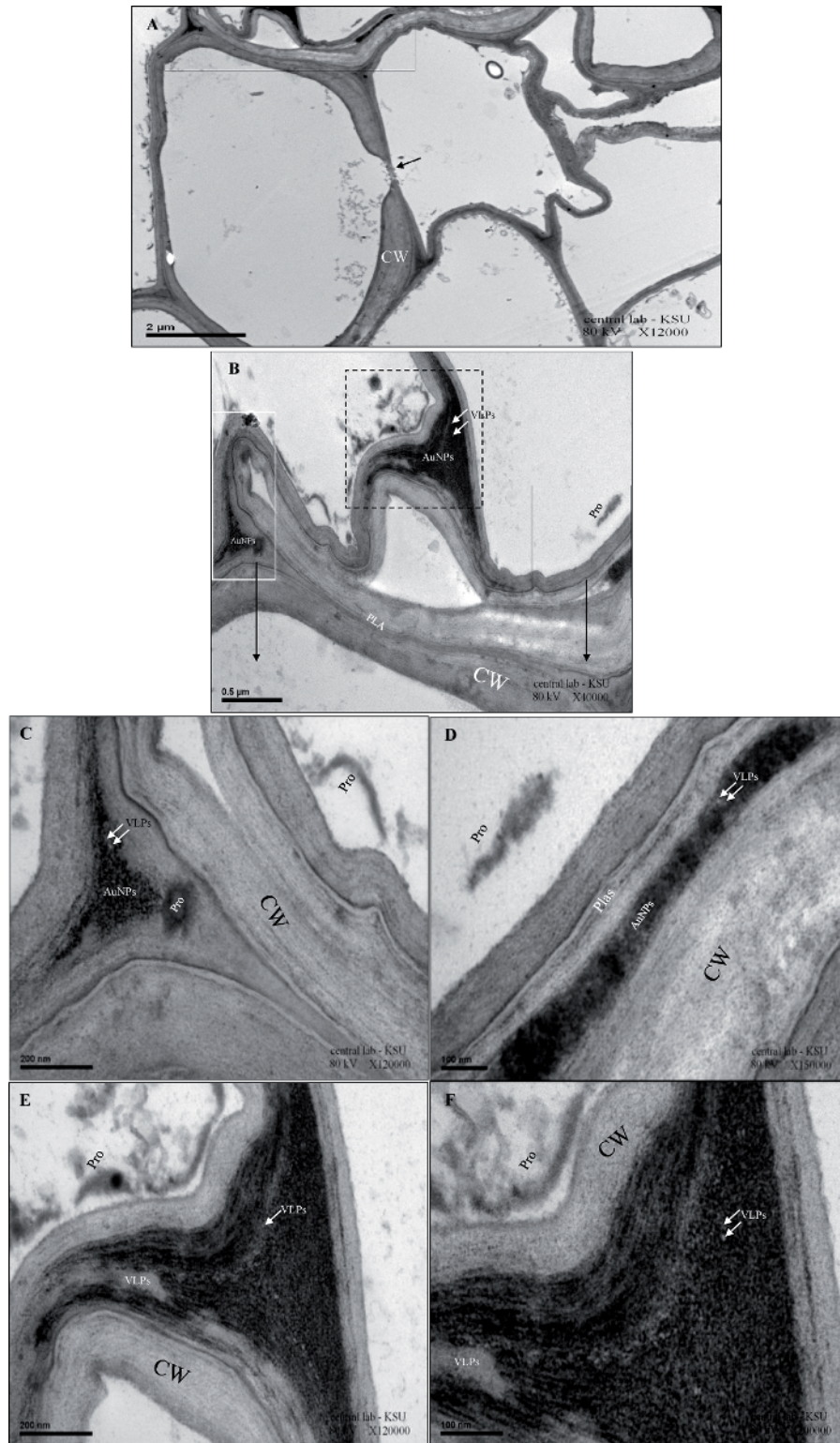


**Figure 4.** Micrographs of the AuNPs integrated inside the cell wall with high density. (A) The cell wall had twisted invaginated shapes as shown in the bold box, and some dynamic move the proteinous material via plasmodesmata (arrow), scale bar 2  $\mu\text{m}$ . (B) Very twisted cell wall as of accumulated dark density AuNPs inside the interaction of their cell wall structure joined with VLPs in three different parts, scale bar 0.5  $\mu\text{m}$ . (C) The AuNPs had low concentration and density with VLPs (white box in B) than in (dashed box in B), scale bar 200 nm. (D) Higher magnification showed high accumulation density of AuNPs with VLPs had very dark color along extended the cell wall in the middle of it (dashed box in B), proteinous contents near the cell wall on the right side (black box in B), scale bar 100 nm. (E and F) VLPs trapped in massive of AuNP inside the cell wall, with higher resolutions, scale bars 200 nm, 100 nm.

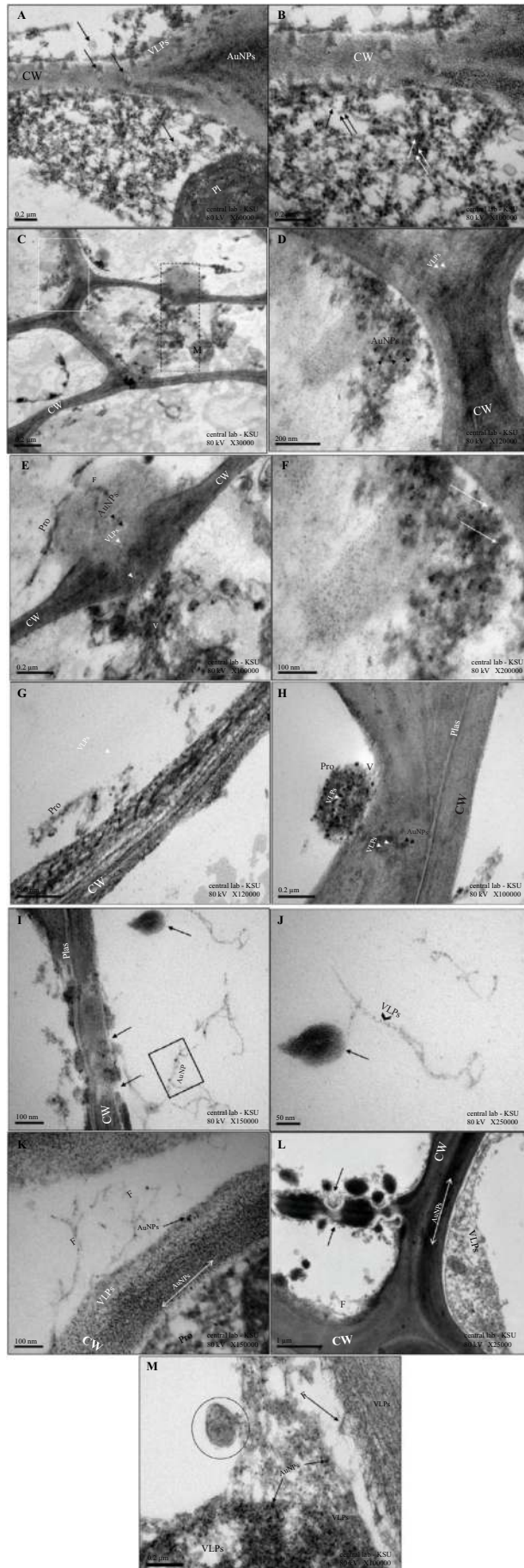


**Figure 5.**

Micrographs of the mechanical transportation of virus through the sieve elements with endosomes. (A) Viral particles associated with AuNPs with endosomes in plasmodesmata connecting with two adjacent parenchyma cells, mechanical transport movement of some vesicles and amorphous inclusions, and filamentous particles stuck or near the cell wall, scale bar 0.2  $\mu\text{m}$ . (B) Mechanical transportation of some blowing VLPs in and out through the cell wall and cytoplasmic membrane compartment (arrows), Nemours AuNPs attracted with deformed VLPs in the cytoplasm, cell wall, and PL. Some empty endosomes exist inside the cytoplasm in the inner part of the cells (arrow), scale bar 0.2  $\mu\text{m}$ . Micrographs of the mechanical transportation of virus through the cell wall with some vesicles, amorphous inclusions, and filamentous particles. (C) The cell is full of many different kinds of abnormal structure endosomes (dashed box) as well as many accumulated and irregular distribution of light and dark area (white box), scale bar 0.5  $\mu\text{m}$ . (D and F) showed the aggregation of VLPs with dark AuNPs near to the cell wall that has intermediate virus particles in the dark area (arrows). Two neighboring cells separated with the cell wall, some cytoplasmic material crossing the cell wall by one of that endosomes to the other cell with VLPs (arrows). Scale bars 200,100 nm. (E) Mechanical transport movement of some vesicles and amorphous inclusions and filamentous particles stuck or near the cell wall. (higher magnification of D), scale bar 0.2  $\mu\text{m}$ . Micrographs of the mechanical transportation of virus through the sieve elements with filamentous strands. (I) Crystalline array (arrow) and some filamentous strands (outlined) in the cytoplasm joined with dark AuNPs; the cell wall has two locations of pits that seem to be the gate of moving materials (arrows), scale bar 100 nm. (J) High magnification for the pseudo-crystal array (arrow) associated with light VLPs (arrow), scale bar 50 nm. (K) Numerous filamentous inclusions extended in the cell lumen toward the cell wall interspersed with AuNPs and VLPs, scale bar 100 nm. (L) Parenchyma cell starts to divide, de-generated cell wall and abnormal deformed cell wall inside the cell (arrows), AuNPs extended along the complete cell wall in high density (arrow with two directions), scale bar 1  $\mu\text{m}$ . (M) Illustrate the endosomes (circular) and filamentous strands near the cell wall, VLPs distributed in the right side and middle of the figure while the AuNPs concentrated in the lower part inside the cytoplasm. Scale bar 0.2  $\mu\text{m}$ .

Two-photon excitation microscopy was used to monitor MWCNTs piercing the cell wall of wheat roots and reaching the cytoplasm [8] without totally entering the cell. After root uptake and penetration of the epidermal cells of Engineered nanomaterials ENMs, transport demand circulation across the root and the xylem. ENMs transported through cell wall pores, the apoplastic pathway, or the symplastic pathway through plasmodesmata, channels that connect neighboring cells around 40 nm in diameter [9]. The uptake and translocation of ENMs in plants are not only related to the particle composition, size, shape, surface properties, but also the type of plant species. Positively charged AuNPs were most readily taken up by plant roots [10], while negatively charged AuNPs most efficiently translocated into stems and leaves from the roots. Higher amounts of the AuNPs accumulated in Radish and ryegrass roots generally than rice and pumpkin roots, as we found in wheat in our study. Utilized AuNPs in that study aggregated to statistically considerable extents in rice shoots; however, none of them depleted in the shoots of radishes and pumpkins. Near, the tissue scale uptake and locative distribution NPs in rice roots and shoots were influenced by the surface charges of Au NPs [11]. Au concentration in rice roots followed the order of AuNP (+) > AuNP (0) > AuNP (–) but with the reversed order for shoots, indicating preferential translocation of negatively charged Au NPs. AuNPs in the xylem within the leaves indicated that the NPS was transported during nutrients and water uptake [12].

Direct penetration of NPS through the cell wall can be envisioned for smaller-size NPS as the pore size on the cell wall (2–20 nm) may limit the passage to the NPs more significant than 20 nm [12]. Furthermore, the cell membrane acts as yet another barrier for an extraneous agent to pass through. To test this hypothesis, [13] investigated uptake and distribution of 3.5 nm or 18 nm-sized citrate-coated AuNPs in tobacco (*Nicotiana Xanthi*), where the authors observed uptake of Au only from 3.5 nm AuNPs treatments [13], distinct with 18 nm-sized AuNPs treatments, and the larger-sized particles adhered to tobacco root surfaces. Also, exposure to 3.5 nm-sized AuNPs resulted in leaf necrosis sustain in plant death. It did not occur with 18 nm AuNPs treatments [13]. On the other hand, a size threshold may happen for NPS translocation to the leaves, which they mentioned to be <36 nm; meanwhile, the accumulation of TiO<sub>2</sub>NPs in the wheat root could only exist if NPs are <140 nm in diameter, with higher aggregation that take place when NPs were much smaller (in the size range 14–22 nm) [14]. Combined, these

observations from chemically different ENMs bolster the premise that particle size could be an essential factor regulating ENM bio uptake in plants.

## Abbreviations

VLPs	Virus-like particles
TMV	Tobacco mosaic virus
MP	Movement protein
AuNPs	Gold nanoparticles
TEM	Transmission electron microscope
DNA	Deoxyribonucleic Acid
mRNAs	Messenger Ribonucleic Acid
MWCNTs	Multi-walled carbon nanotubes
NLS	Nuclear Localization Signal Peptide;
ENMs	Engineered nanomaterials
NPS	Nanoparticles
nm	NanoMeter
PL	Plastid
CW	Cell Wall
M	Mitochondria
S	Starch
(BYDV-PAV)	Barley Yellow Dwarf Virus
PLA	Plasmodesmata
PRO	Proteinous
F	Filamentous
V	Vesicles

## Author details


Noorah Abdulaziz Othman Alkubaisi<sup>1\*</sup> and Nagwa Mohammed Amin Aref<sup>2</sup>

<sup>1</sup> Department of Botany and Microbiology, College of Science, Female Scientific and Medical Colleges, King Saud University, Riyadh, Kingdom of Saudi Arabia

<sup>2</sup> Faculty of Agriculture, Department of Microbiology, Ain Shams University, Muhafazat al Qahirah, Cairo, Egypt

\*Address all correspondence to: [nalkubaisi@ksu.edu.sa](mailto:nalkubaisi@ksu.edu.sa)

## IntechOpen

© 2021 The Author(s). Licensee IntechOpen. Distributed under the terms of the Creative Commons Attribution - NonCommercial 4.0 License (<https://creativecommons.org/licenses/by-nc/4.0/>), which permits use, distribution and reproduction for non-commercial purposes, provided the original is properly cited. 

## References

- [1] A. Comeau, S. Haber, Breeding for BYDV tolerance in wheat as a basis for a multiple stress tolerance strategy, *Barley Yellow Dwarf Disease: Recent Advances and Future Strategies* (2002) 82.
- [2] E. Neumann, A. Sprafke, E. Boldt, H. Wolf, Biophysical considerations of membrane electroporation, *Guide to electroporation and electrofusion* (1992) 77-90.
- [3] K.N. Thakkar, S.S. Mhatre, R.Y. Parikh, Biological synthesis of metallic nanoparticles, *Nanomedicine: nanotechnology, biology, and medicine* 6(2) (2010) 257-262.
- [4] J. Nari, G. Noat, JJB Ricard, Pectin methylesterase, metal ions, and plant cell-wall extension. Hydrolysis of pectin by plant cell-wall pectin methylesterase, 279(2) (1991) 343-350.
- [5] A. Fleischer, M.A. O'Neill, R. Ehwald, The pore size of non-graminaceous plant cell walls is rapidly decreased by borate ester cross-linking of the pectic polysaccharide rhamnogalacturonan II, *Plant Physiology* 121(3) (1999) 829-838.
- [6] H.-M. Chen, L.-T. Chen, K. Patel, Y.-H. Li, D.C. Baulcombe, S.-H. Wu, 22-Nucleotide RNAs trigger secondary siRNA biogenesis in plants, *Proceedings of the National Academy of Sciences* 107(34) (2010) 15269-15274.
- [7] D.S. Goldfarb, J. Gariépy, G. Schoolnik, R.D. Kornberg, Synthetic peptides as nuclear localization signals, *Nature* 322(6080) (1986) 641-644.
- [8] E. Wild, K.C. Jones, Novel method for the direct visualization of in vivo nanomaterials and chemical interactions in plants, *Environmental Science & technology* 43(14) (2009) 5290-5294.
- [9] LG Tilney, T.J. Cooke, P.S. Connelly, MS Tilney, The structure of plasmodesmata as revealed by plasmolysis, detergent extraction, and protease digestion, *Journal of Cell Biology* 112(4) (1991) 739-747.
- [10] Z.-J. Zhu, H. Wang, B. Yan, H. Zheng, Y. Jiang, O.R. Miranda, V.M. Rotello, B. Xing, R.W. Vachet, Effect of surface charge on the uptake and distribution of gold nanoparticles in four plant species, *Environmental Science & Technology* 46(22) (2012) 12391-12398.
- [11] J. Koelmel, T. Leland, H. Wang, D. Amarasiriwardena, B. Xing, Investigation of gold nanoparticles uptake and their tissue level distribution in rice plants by laser ablation-inductively coupled-mass spectrometry, *Environmental pollution* 174 (2013) 222-228.
- [12] G. Zhai, K.S. Walters, D.W. Peate, P.J. Alvarez, J.L. Schnoor, Transport of gold nanoparticles through plasmodesmata and precipitation of gold ions in woody poplar, *Environmental science & technology letters* 1(2) (2014) 146-151.
- [13] T. Sabo-Attwood, J.M. Unrine, J.W. Stone, C.J. Murphy, S. Ghoshroy, D. Blom, P.M. Bertsch, L.A. Newman, Uptake, distribution and toxicity of gold nanoparticles in tobacco (*Nicotiana Xanthi*) seedlings, *Nanotoxicology* 6(4) (2012) 353-360.
- [14] C. Larue, J. Laurette, N. Herlin-Boime, H. Khodja, B. Fayard, A.-M. Flank, F. Brisset, M. Carriere, Accumulation, translocation and impact of TiO<sub>2</sub> nanoparticles in wheat (*Triticum aestivum* spp.): influence of diameter and crystal phase, *Science of the total environment* 431 (2012) 197-208.